

Synthesis of 2-Pyridyl-benzimidazole Iridium(III), Ruthenium(II), and Platinum(II) Complexes. Study of the Activity as Inhibitors of Amyloid- β Aggregation and Neurotoxicity Evaluation

Gorakh S. Yellol,[†] Jyoti G. Yellol,[†] Vijaya B. Kenche,[‡] Xiang Ming Liu,[‡] Kevin J. Barnham,^{*,‡} Antonio Donaïre,[†] Christoph Janiak,[§] and José Ruiz^{*,†}

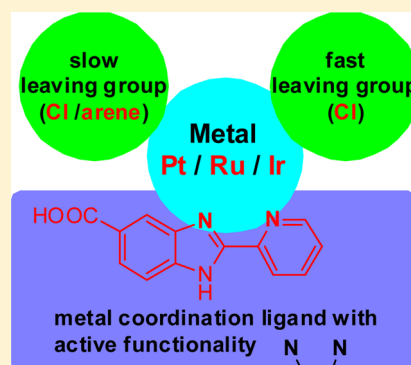
[†]Departamento de Química Inorgánica and Regional Campus of International Excellence (Campus Mare Nostrum), Universidad de Murcia and Instituto Murciano de Investigación Biosanitaria IMIB-Arrixaca, E-30071 Murcia, Spain

[‡]The Florey Institute of Neuroscience and Mental Health, The University of Melbourne, Parkville 3016, Australia

[§]Institut für Anorganische Chemie und Strukturchemie, Universität Düsseldorf, D-40204 Düsseldorf, Germany

Supporting Information

ABSTRACT: The design of small molecules that can target the aggregation of $A\beta$ as potential therapeutic agents for Alzheimer's disease is an area of study that has attracted a lot of attention recently. The novel ligand methyl 1-butyl-2-pyridyl-benzimidazole carboxylate was prepared for the synthesis of a series of new iridium(III), ruthenium(II), and platinum(II) 2-pyridyl-benzimidazole complexes. The crystal structure of the half-sandwich iridium(III) complex was established by X-ray diffraction. An arrangement of two cationic complexes in the unit cell is observed, and it seems to be organized by weak $\pi\cdots\pi$ interactions that are taking place between two symmetry-related benzimidazole ring systems. All new compounds inhibited aggregation of $A\beta$ 1–42 in vitro as shown by both thioflavin T fluorescence assay and transmission electron microscopy. Among them the Ir compound rescued the toxicity of $A\beta$ 1–42 in primary cortical neurons effectively.



INTRODUCTION

A century after the first report, the development of effective treatment of Alzheimer disease (AD) remains challenging (www.alz.org), and presently, there is no cure for this disease that worsens progressively and eventually leads to death within a few years. Also, for example, the health cost in the U.S. is much higher for AD than it is for cardiovascular diseases and cancer. Extracellular amyloid plaques with main constituent of amyloid β -peptide ($A\beta$) and neurofibrillary tangles composed of hyperphosphorylated tau protein are key pathological indicators.¹ Recent research proposes that the aggregation of $A\beta$ drives the disease process as various forms of aggregated $A\beta$ have been revealed to be toxic.² As a result, the development of a variety of therapeutic strategies targeting $A\beta$ have been stimulated. One approach is to design bifunctional molecules that can chelate the metal out of $A\beta$ and control or modulate its aggregation.³ Another very different approach is to use metal complexes that can modulate $A\beta$ aggregation,⁴ $A\beta$ containing a metal-binding motif near the *N* terminus. Taking advantage of this metal-binding ability, substantial efforts have been dedicated to develop metal-based anti-Alzheimer compounds targeting $A\beta$.^{5,6} Metal-organic compounds could solve many of the challenges in turning a structural lead into a drug candidate with improved efficacy and tolerability as they are suitable for rational drug design. In a pioneering study, Barnham et al. proved that platinum complexes strongly inhibit amyloid

oligomerization and attenuate its neurotoxicity in vitro.⁷ Moreover, a few subsequent studies with other metal compounds nicely corroborated the feasibility of such a strategy.⁴ However, there are some critical factors that must be clarified for effective development of metal-based inhibitors of β -amyloid aggregation. First of all, the evaluation of the neurotoxicity of these compounds is strictly required with respect to its ligand, metal, and their combination. Subsequently, it would be extremely important to evaluate the capability of metal compounds to cross the blood-brain barrier.

In this context, our study focused on evaluating the effect of the type of metal on its ability to inhibit aggregation of $A\beta$ and its neurotoxicity.^{8–11} Recently some platinum, ruthenium, and iridium metal complexes have shown promising activity as inhibitors of amyloid- β in their independent studies.^{4,12–14} Therefore, it was determined to study the inhibition of aggregation of $A\beta$ 1–42 in vitro of these precious metals keeping the basic core ligand.

Here we disclose novel platinum, ruthenium, and iridium benzimidazole complexes with activity as inhibitors of aggregation of amyloid- β along with their toxicity profiles. The designed concept of the present metal complexes has

Received: August 31, 2014

Published: November 19, 2014

originated from our recent study of similar benzimidazole anticancer compounds and the recognition of the biological role of the benzimidazoles, which exhibit a wide range of pharmacological properties.^{15–22}

RESULTS AND DISCUSSION

Molecular Design. As shown in Figure 1, the typical active N–N functionality embedded in pyridyl–benzimidazole will

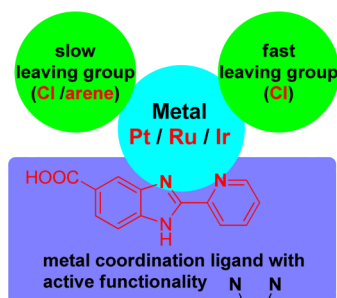


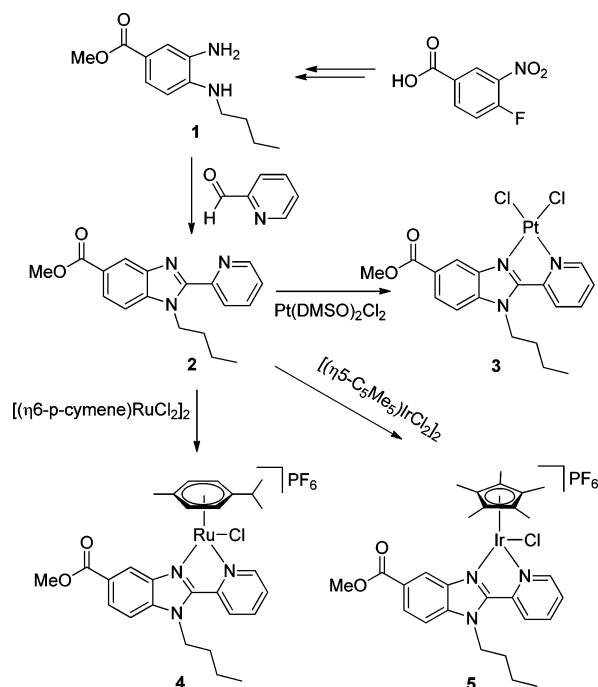
Figure 1. Design of the 2-pyridyl-benzimidazole ligand for preparation of metallodrugs.

serve as a basic core ligand with a readily available metalation site. NH-functionality features an installation of different moieties to modulate lipophilicity/hydrophilicity. The carboxyl functionality is required to tune the design with the goal that it serves as a handle for the intended functionalization of metallodrugs with diverse moieties to explore their ability to cross the blood-brain barrier.

The designed molecule was synthesized using our developed strategy reported earlier.¹⁵ Accordingly, key intermediate **1** was synthesized from 4-fluoro-3-nitro-benzoic acid by acid catalyzed methyl esterification, nucleophilic aromatic substitution of a fluoro group by butyl amine, and subsequent reduction of a nitro group using zinc and ammonium formate in methanol in 60% overall yield (Scheme 1). Aiming to tune the lipophilicity of the final complex, a butyl group attached to the NH functionality was the first choice. The core scaffold **2** was synthesized by condensation of **1** and 2-pyridinecarboxaldehyde in acidic ethanol at room temperature in good yield and confirmed by spectroscopic methods (see Supporting Information).

Synthesis of the New Metal Compounds. Compound **3** was prepared by treating pyridyl–benzimidazole **2** with an equimolar mixture of $\text{Pt}(\text{DMSO})_2\text{Cl}_2$ (DMSO = dimethyl sulfoxide) at room temperature for 24 h (Scheme 1). Formation of complex **3** was confirmed by NMR spectroscopic and electrospray ionization mass spectrometric (ESI-MS) methods. Ligand **2** was also treated with *para*-cymene ruthenium(II) $[(\eta^6\text{-}p\text{-cymene})\text{RuCl}_2]_2$ in methanol at room temperature to obtain, after addition of Bu_4NPF_6 , the ruthenium cationic complex **4** in 72% yield. Formation of the ruthenium complex was confirmed by spectroscopic methods. In the ^1H NMR spectrum of **4** introduction of four doublets at 6.5–6.7 ppm, a singlet at 2.2 ppm, and two doublets at 0.9 ppm for six protons corresponding to *p*-cymene depicts the formation of ruthenium complex **4**. Similarly, the half-sandwich iridium(III) complex **5** was prepared using a similar method starting from the corresponding pentamethylcyclopentadienyl chlorido iridium(III) dimer in good yield. Again formation of **5** was confirmed by spectroscopic and analytical methods,

Scheme 1. Synthesis of Methyl 1-Butyl-2-pyridyl-benzimidazole Carboxylate Pt(II)/Ru(II)/Ir(III) Complexes



including COSY, NOESY, and HSQC NMR techniques (Supporting Information, Figures S1–S3).

X-ray Crystal Structure of Complex 5·CH₂Cl₂. The crystal structure of the iridium complex **5·CH₂Cl₂** was established by X-ray diffraction (Figure 2, Table 1, and

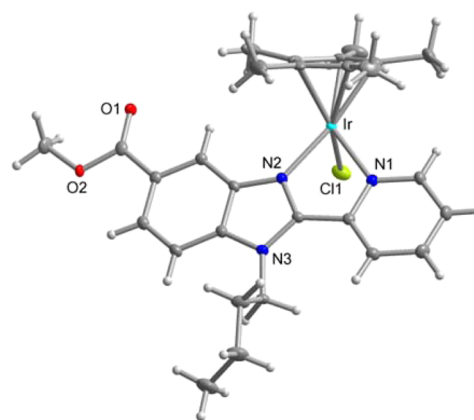


Figure 2. X-ray crystallographic ORTEP diagram of the cation of complex **5·CH₂Cl₂**. Selected bond lengths (Å) and angles (deg): Ir–Cl1 = 2.3929(4), Ir–N1 = 2.1208(15), Ir–N2 = 2.0809(14), Ir–Cp(centroid) = 1.7903(8), Cl1–Ir–N2 = 85.32(4), Cl1–Ir–N1 = 85.93(4), N1–Ir–N2 = 75.08(6).

Supporting Information, Tables S1–S4). Figure 2 depicts the ORTEP diagram of the cation of complex **5**, confirming its “piano-stool” structure with the pentamethylcyclopentadienyl group displaying the common η^5 coordination mode, whereas the 1-butyl-2-pyridyl-benzimidazole carboxylate assumes a bidentate-chelate coordination mode ($\kappa^2\text{-}N,N$), the two rings of the benzimidazole and phenyl moieties being not strictly coplanar. The Ir–N distance is shorter for the benzimidazole heterocycle than it is for the pyridyl moiety.

Table 1. Crystal Structure Determination Details of **5**·CH₂Cl₂

	5 ·CH ₂ Cl ₂
chemical formula	C ₂₈ H ₃₄ ClIrN ₃ O ₂ F ₆ P·CH ₂ Cl ₂
fw [g/mol]	902.13
cryst system	triclinic
<i>a</i> [Å]	8.3118(4)
<i>b</i> [Å]	11.8165(5)
<i>c</i> [Å]	16.9769(8)
α [deg]	91.208(1)
β [deg]	90.048(1)
γ [deg]	100.290(1)
<i>V</i> [Å ³]	1640.21(13)
temp (K)	100(2)
space group	<i>P</i> $\bar{1}$
<i>Z</i>	2
μ [mm ⁻¹]	4.43
reflcs colcd	65 066
inpdnt reflcs	10 041
<i>R</i> (int)	0.039
restraints/params	0/430
GOF on <i>F</i> ²	1.059
<i>R</i> ₁ / <i>wR</i> ₂ [<i>I</i> > 2 σ (<i>I</i>)]	0.0184/0.0422
<i>R</i> ₁ / <i>wR</i> ₂ (all reflcs)	0.0203/0.0428

The complex **5** exhibits a CH₂Cl₂ molecule (Supporting Information, Figure S4) in the crystal lattice.

The unit cell of compound **5**·CH₂Cl₂ contains two molecular units (Supporting Information, Figure S5). The overall crystal packing is largely dominated by Coulomb interactions between the (pentamethylcyclopentadienyl)-(methyl 1-butyl-2-pyridyl-benzimidazole carboxylate)-chlorido-iridium(III) cation and the PF₆ anion. No C–H... π , and few significant C–H...Cl and C–H...F interactions (Supporting Information, Table S5) are indicated by PLATON.²³ In view of the disorder in the PF₆ anion (Supporting Information, Figure S6) we would, however, not assign too much significance to the C–H...F interactions. The arrangement of the two cations in the unit cell seems to be organized by weak π ... π interactions, which are depicted in Figure 3 and Supporting Information, Figure S6 and are detailed in Table S6 (Supporting Information). The π ... π interactions take place between two symmetry-related benzimidazole ring systems.^{24,25}

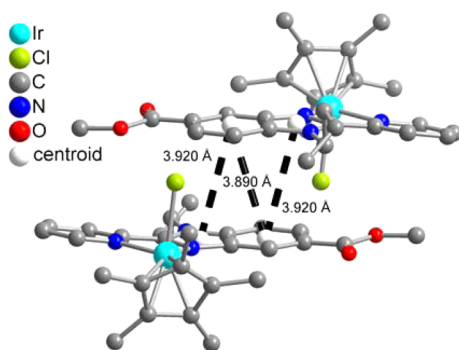


Figure 3. π ... π interactions with their centroid–centroid contacts between two (pentamethylcyclopentadienyl)-(methyl 1-butyl-2-pyridyl-benzimidazole carboxylate)-chlorido-iridium(III) cation in compound **5**·CH₂Cl₂.

Biological Activity: Inhibition of Amyloid Aggregation Studies. All three compounds were tested for their ability to inhibit amyloid aggregation of A β 42 using a thioflavin T fluorescence assay.¹ The results indicated that 1 μ M of all three compounds was sufficient to inhibit A β amyloid aggregation (Figure 4). Inhibition of amyloid formation was confirmed by transmission electron microscopy as shown in Figure 5.

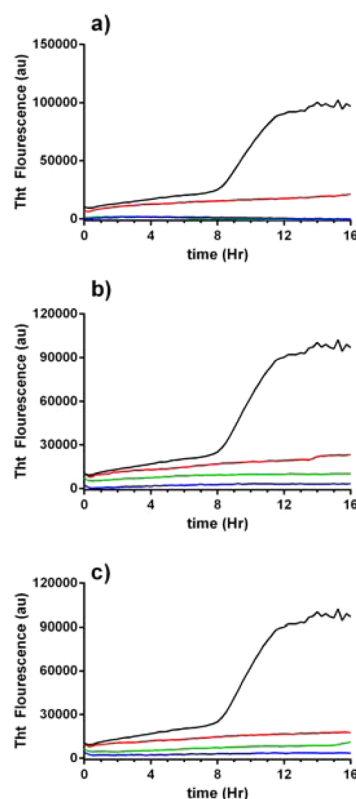


Figure 4. Inhibition of A β 42 aggregation by (a) **3**, (b) **4**, and (c) **5**. A β 42 (10 μ M) was incubated at 37 °C in PBS buffer (pH 7.4) along with varying concentrations of test compounds and ThT (20 μ M). Dose response curves representing A β 42 alone (black), 20 μ M (blue), 10 μ M (green), and 1 μ M (red) were shown in the ThT assay (*n* = 2). All the compounds showed inhibition of A β 42 aggregation.

Rescue of A β Neurotoxicity. To ascertain whether the inhibition of amyloid resulted in the rescue of A β neurotoxicity, primary cortical neurons were treated with A β in the absence or presence of the three diamagnetic compounds (Figure 6). At 10 μ M A β on its own is toxic to the cells. Co-treatment with compound **3** shows a marginal nonsignificant rescue of A β -induced neurotoxicity; the labile compound **4** is itself toxic and therefore unable to rescue A β toxicity. The more inert compound **5** exhibited a robust rescuing of A β neurotoxicity. A proof of the different kinetic behavior of the Ru and the Ir compounds is that **4** (Ru) reacts readily with aqueous medium as shown by ¹H NMR (Supporting Information, Figure S7). After the adequate functionalization to make complex **5** able to cross the blood-brain barrier or to make complex **5** bioavailable, this iridium compound can be a good candidate for *in vivo* studies.

CONCLUSIONS

We have successfully synthesized a novel methyl 1-butyl-2-pyridyl-benzimidazole carboxylate ligand and a new series of

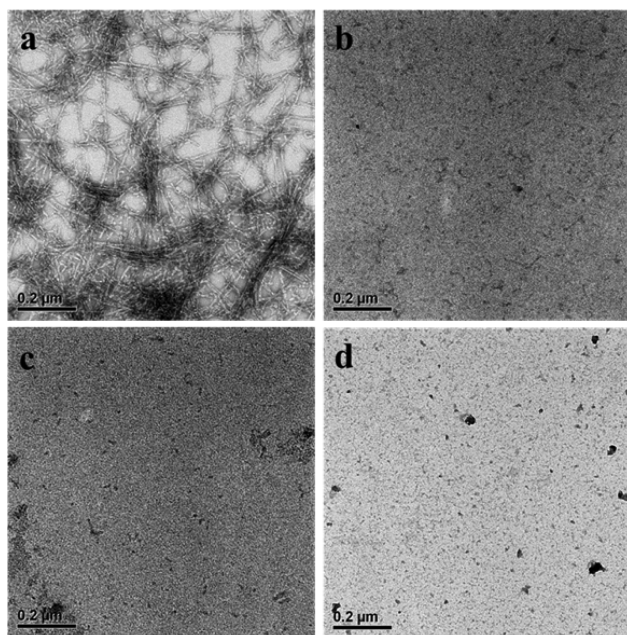


Figure 5. Inhibition of $A\beta_{42}$ aggregation: Electron micrographs of $A\beta_{42}$ ($10\ \mu\text{M}$) incubated at $37\ ^\circ\text{C}$ for 16 h, (a) $A\beta_{42}$ alone, (b) with complex 3 ($10\ \mu\text{M}$), (c) with complex 4 ($10\ \mu\text{M}$), (d) with complex 5 ($10\ \mu\text{M}$).

novel 2-pyridyl-benzimidazole precious metal complexes. The crystal structure of the half-sandwich complex **5** shows that the Ir–N distance is shorter for the benzimidazole heterocycle than it is for the pyridyl moiety. Also weak $\pi\cdots\pi$ interactions are observed that are taking place between two symmetry-related benzimidazole ring systems. All new compounds inhibited aggregation of $A\beta_{1-42}$ in vitro as shown by both thioflavin T fluorescence assay and transmission electron microscopy. Ir complex **5** rescued the toxicity of $A\beta_{1-42}$ in primary cortical neurons effectively.

EXPERIMENTAL SECTION

Instrumental Measurements. The C, H, and N analyses were performed with a Carlo Erba model EA 1108 microanalyzer. The ^1H and ^{13}C NMR spectra were recorded on a Bruker AC 300E or a Bruker AV 400 spectrometer. Chemical shifts are cited relative to SiMe_4 (^1H and ^{13}C , external). ESI mass (positive mode) analyses were performed on a HPLC/MS TOF 6220. UV–vis spectroscopy was carried out on a PerkinElmer Lambda 750 S spectrometer with operating software. Fluorescence measurements were carried out with a PerkinElmer LS 55 50 Hz Fluorescence Spectrometer.

Materials. Solvents were dried by the usual methods. K_2PtCl_4 , $[(\eta^6\text{-cymene})\text{RuCl}_2]_2$, $[(\eta^5\text{-C}_5\text{Me}_5)\text{IrCl}_2]_2$, were obtained from Sigma-Aldrich (Madrid, Spain); $\text{Pt}(\text{DMSO})_2\text{Cl}_2$ was prepared using reported procedure.²⁶

Preparation of Compound 1. Methyl 4-fluoro-3-nitrobenzoate (1 mmol) was dissolved in dichloromethane (10 mL) in round-bottom flask equipped with stirrer and nitrogen atmosphere. Butyl amine (2 mmol) was added to it at room temperature with constant stirring followed by addition of triethylamine (2 mmol). The reaction mixture was stirred at room temperature for 12 h, and the progress of reaction was monitored by thin-layer chromatography (TLC). After complete conversion, reaction was quenched by water (10 mL), and product was extracted by dichloromethane ($2 \times 10\ \text{mL}$). The combined dichloromethane layer was washed with water (10 mL) and brine (10 mL), dried on sodium sulfate, and concentrated under reduced pressure. The crude product was purified by column chromatography using ethyl acetate–hexane (1:5) as eluent to get methyl 4-

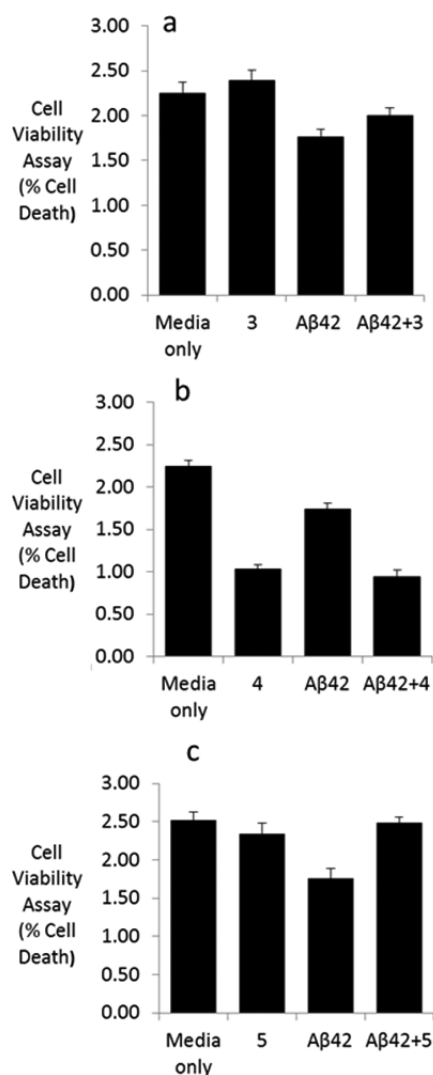


Figure 6. Inhibition of $A\beta_{42}$ toxicity. Cell viability of primary cortical neurons treated with $A\beta_{42}$ for 4 d was measured by MTS absorbance at 490 nm. (a) $A\beta$ treatment reduces cell viability that is rescued by coinubation of $A\beta_{42}$ with complex 3. (b) Complex 4 itself is toxic to the cells, and its coinubation with $A\beta_{42}$ resulted in a negative effect. (c) Complex 5 showed rescue of cell death from $A\beta_{42}$ toxicity. “Media only” is the DMSO negative control.

(butylamino)-3-nitrobenzoate in 79% yield. Subsequently, methyl 4-(butylamino)-3-nitrobenzoate (1 mmol) was dissolved in methanol (10 mL) in a round-bottom flask equipped with a stirrer and nitrogen atmosphere. Zinc (3 mmol) was added at room temperature with constant stirring followed by addition of ammonium formate (2 mmol) in two batches. The reaction mixture was stirred at room temperature for 5 h, and the progress of reaction was monitored by TLC. After complete conversion, reaction was filtered to remove zinc and unreacted ammonium formate. Filtrate was concentrated and then dissolved in dichloromethane and stirred for 30 min. The undissolved material was removed by filtration, and dichloromethane was concentrated under reduced pressure. The crude product was purified by column chromatography using ethyl acetate–hexane (1:2) as eluent to get methyl 3-amino-4-(butylamino)benzoate (**1**) in 68% yield.

Preparation and Characterization of Compound 2. Methyl 3-amino-4-(butylamino)benzoate **1** (1.0 mmol) was dissolved in ethanol (10 mL) in round-bottom flask equipped with stirrer and nitrogen atmosphere. 2-Pyridinecarboxaldehyde (1.0 mmol) was added at room temperature with constant stirring followed by addition of trifluoroacetic acid (0.1 mmol) and magnesium sulfate (5 mmol). The reaction

mixture was stirred at room temperature for 24 h, and the progress of reaction was monitored by TLC. After complete conversion, reaction was filtered to remove magnesium sulfate. Filtrate was concentrated and then dissolved in dichloromethane. Dichloromethane was washed with water (2 × 10 mL) and brine (10 mL), dried on sodium sulfate, and concentrated under reduced pressure. The crude product was purified by column chromatography using ethyl acetate–hexane (1:3) as eluent to obtain methyl 1-butyl-2-(pyridin-2-yl)-1H-benzo[d]imidazole-5-carboxylate (**2**) in 57% yield. M_r ($C_{18}H_{19}N_3O_2$) = 309.1477 g/mol. Anal. Calcd for $2 C_{18}H_{19}N_3O_2$: C, 69.88; H, 6.19; N, 13.58. Found: C, 70.12; H, 6.56; N, 13.27%. 1H NMR (400.13 MHz, $CDCl_3$) δ 0.94 (t, 3H, $J = 7.3$ Hz), 1.32–1.42 (m, 2H), 1.82–1.92 (m, 3H), 3.96 (s, 3H), 4.07 (t, 2H, $J = 7.2$ Hz), 7.38–7.42 (m, 1H), 7.50 (d, 1H, $J = 8.5$ Hz), 7.90 (m, 1H), 8.08 (dd, 1H, $J = 1.5$ Hz, $J = 7.0$ Hz), 8.52 (d, 1H, $J = 7.8$ Hz), 8.60 (s, 1H), 8.72 (d, 1H, $J = 4.4$ Hz); ^{13}C NMR (100.60 MHz, $CDCl_3$) δ 167.5, 151.5, 150.2, 148.6, 142.1, 139.8, 136.8, 124.8, 124.5 (2 C), 124.0, 122.4, 109.8, 52.0, 45.5, 32.1, 19.9, 213.6; Positive-ion ESI mass spectra (DMSO) at $m/z = 310.1552 [M + H]^+$.

Preparation and Characterization of Compound 3. Methyl 1-butyl-2-(pyridin-2-yl)-1H-benzo[d]imidazole-5-carboxylate **2** (1 mmol) was dissolved in freshly distilled dichloromethane in a dry round-bottom flask equipped with stirrer and nitrogen atmosphere. Sodium acetate (1.2 mmol) was added to this at room temperature with constant stirring followed by addition of $Pt(DMSO)_2Cl_2$ (0.5 mmol). The reaction mixture was stirred at room temperature for 24 h. The precipitate formed was filtered and washed with dichloromethane and diethyl ether, respectively. The yellowish color platinum complex **3** was obtained in good yield (77%). M_r ($C_{18}H_{19}Cl_2N_3O_2Pt$) = 574.0502 g/mol. Anal. Calcd for $C_{18}H_{19}Cl_2N_3O_2Pt$: C, 37.58; H, 3.33; N, 7.30; Found: C, 37.88; H, 3.50; N, 7.41%. 1H NMR (400.13 MHz, $CDCl_3$) δ 9.64–9.66 (m, 2H), 8.45 (dt, 1H, $J = 8.0$, 1.4 Hz), 8.35 (d, 1H, $J = 8.0$ Hz), 8.10–8.11 (m, 2H), 7.85 (t, 1H, $J = 7.2$ Hz), 4.83 (t, 1H, $J = 7.4$ Hz), 3.90 (s, 3H), 1.85 (quint, 2H, $J = 7.4$ Hz), 1.44–1.39 (m, 2H), 0.89 (t, 3H, $J = 7.4$ Hz); ^{13}C NMR (100.60 MHz, $CDCl_3$) δ 199.90, 157.41, 150.02, 141.53, 138.54, 137.85, 137.26, 125.27, 124.98, 124.29, 120.90, 118.61, 115.12, 51.53, 49.44, 33.15, 20.16, 13.87; Positive-ion ESI mass spectra ion cluster (DMSO) at $m/z = 568.0857 [M + H_2O]^+$.

Preparation and Characterization of Compound 4. Methyl 1-butyl-2-(pyridin-2-yl)-1H-benzo[d]imidazole-5-carboxylate **2** (1.0 mmol) was dissolved in freshly distilled methanol (30 mL) in a dry round-bottom flask equipped with stirrer and nitrogen atmosphere. $[(\eta^6\text{-cymene})RuCl_2]_2$ (0.5 mmol) was added at room temperature with constant stirring. The reaction mixture was stirred at room temperature for the next 15 h. The yellow solution was concentrated to 15 mL, and Bu_4NPF_6 (1.0 mmol) was added in it. The reaction mixture was stirred at room temperature for the next 30 min to furnish yellow precipitate, which was filtered and washed with methanol and diethyl ether. The yellow crystalline ruthenium complex **3** was obtained in good yield (85%). M_r ($C_{28}H_{33}ClF_6N_3O_2PRu$) = 725.0947 g/mol. Anal. Calcd for $C_{28}H_{33}ClF_6N_3O_2PRu$: C, 46.38; H, 4.59; N, 5.80; Found: C, 46.71; H, 4.33; N, 6.03%. 1H NMR (400.13 MHz, $CDCl_3$) δ 0.96 (t, 3H, $J = 7.3$ Hz), 1.05–1.08 (m, 6H), 1.42–1.49 (m, 2H), 1.86–1.96 (m, 2H), 2.22 (s, 3H), 2.62–2.71 (m, 1H), 4.05 (s, 3H), 4.59–4.83 (m, 2H), 5.82 (d, 1H, $J = 6.5$ Hz), 5.90 (d, 1H, $J = 6.5$ Hz), 6.03 (d, 1H, $J = 5.5$ Hz), 6.10 (d, 1H, $J = 5.9$ Hz), 7.67–7.70 (m, 2H), 8.14–8.23 (m, 2H), 8.26–8.29 (dd, 1H, $J = 1.5$ Hz, $J = 7.3$ Hz), 8.54 (s, 1H), 9.54 (d, 1H, $J = 5.5$ Hz); ^{13}C NMR (100.60 MHz, $CDCl_3$) δ 166.02, 157.47, 150.11, 145.11, 140.17, 139.86, 139.02, 128.08, 127.82, 127.49, 124.62, 119.90 (4C), 112.02, 85.94, 84.20, 83.18, 81.29, 52.72, 46.23, 31.51, 31.20, 21.99, 19.90, 18.75, 13.52; Positive-ion ESI mass spectra ion cluster (DMSO) at $m/z = 580.1308 [M - PF_6]^+$.

Preparation and Characterization of Compound 5. Methyl 1-butyl-2-(pyridin-2-yl)-1H-benzo[d]imidazole-5-carboxylate **2** (1 mmol) was dissolved in freshly distilled methanol (30 mL) in a dry round-bottom flask equipped with stirrer and nitrogen atmosphere. $[(\eta^5\text{-}C_5Me_5)IrCl_2]_2$ (0.5 mmol) was added at room temperature with constant stirring. The reaction mixture was stirred at room

temperature for the next 15 h. The yellow solution was concentrated to 15 mL, and Bu_4NPF_6 (1.0 mmol) was added to it. The reaction mixture was stirred at room temperature for the next 30 min to furnish yellow precipitate, which was filtered and washed with methanol and diethyl ether. The yellow crystalline iridium complex **5** was obtained in good yield (87%). M_r ($C_{28}H_{33}ClF_6N_3O_2PRu$) = 817,1611 g/mol. Anal. Calcd for $C_{28}H_{33}ClF_6N_3O_2P$: C, 41.15; H, 4.19; N, 5.14; Found: C, 41.34; H, 4.07; N, 5.20%. 1H NMR (400.13 MHz, $CDCl_3$) δ 8.98 (d, $J = 5.0$ Hz, 1H), 8.55 (s, 1H), 8.32 (d, $J = 8.0$ Hz, 1H), 8.21–8.25 (m, 1H), 7.73 (t, $J = 6.4$ Hz, 1H), 7.67 (d, $J = 8.9$ Hz, 1H), 4.94–5.02 (m, 1H), 4.63–4.71 (m, 1H), 4.02 (s, 3H), 1.94–1.97 (m, 2H), 1.77 (s, 15H), 1.53–1.58 (m, 2H), 1.02 (t, $J = 7.3$ Hz, 3H); ^{13}C NMR (100.60 MHz, $CDCl_3$) δ 166.0, 152.6 (2C), 145.8, 139.2, 137.4 (2C), 128.4, 127.4 (2C), 127.2, 125.1, 119.7, 112.2, 89.2 (5C), 52.6, 31.5, 20.0, 13.5, 9.2 (5C); Positive-ion ESI mass spectra ion cluster (DMSO) at $m/z = 672.1938 [M - PF_6]^+$.

X-ray Crystal Structure Analysis. Suitable crystals of **5** were grown from dichloromethane/hexane. Crystal data, data collection, and structure refinement details are summarized in Supporting Information, Table S1. Hydrogen atoms for aromatic CH, aliphatic CH, CH_2 , and methyl groups were positioned geometrically ($C-H = 0.95$ Å for aromatic CH, $C-H = 1.00$ Å for aliphatic CH, $C-H = 0.99$ Å for CH_2 , $C-H = 0.98$ Å for CH_3) and refined using a riding model (AFIX 43 for aromatic CH, AFIX 23 for CH_2 , AFIX 137 for rotating group for CH_3), with $U_{iso}(H) = 1.2U_{eq}(CH)$ and $U_{iso}(H) = 1.5U_{eq}(CH_3)$.

The PF_6^- anion is rotationally disordered around the F5–P–F6 axis (see Supporting Information, Figure S4). Two sets of F1–F4 positions in the square plane could be refined with PART commands. The major component F1–F4 has an ~80% occupation, while F1b–F4b are occupied to 20%. The minor F1b–F4b were refined isotropically.

In Situ ThT Fluorescence Assay for $A\beta$ Aggregation.

Compounds to be tested were dissolved at 400, 200, and 20 μM in 100% DMSO stock solution. The final DMSO concentration was 5%. Each sample (500 μL) was prepared using the appropriate concentration of compound (25 μL), $A\beta 42$ (100 μM of 50 μL), and ThT (20 μM of 425 μL) and pipetted out in 150 μL aliquots into three wells of black bottom clear 96-microwell plate. The plate was sealed to prevent evaporation and was put into the plate reader (BMG Labtechnologies), which was then set to incubate at 37 °C for 16 h. The ThT fluorescence was recorded at every 15 min (with 10 s of orbital shaking) interval via bottom reading with excitation at 440 and emission at 490 nm.

Electron Microscopy. Electron microscopy was performed to confirm the effect of test compounds on formation of any aggregates/fibrils and to observe any possible morphological changes. Aliquots were collected from the assay samples at the end of incubation for imaging. EM carbon-coated gold grids (ProSciTech, Kirwan, Australia) were glow-discharged (Brodsky et al., 1977) and coated (carbon-coated side up) with 20 μM of assay samples. The grids were then blotted with filter paper to remove excess solvent, washed quickly with 10 μL of mH_2O , blotted, and negatively stained with 10 μL of 1.5% (w/v) uranyl acetate (UA) for 20 s. Grids were then blotted again and air-dried before analysis. Images were taken using a Tecnai G2 transmission electron microscope (TEM) (FEI, Hillsboro, OR, U.S.) operating at 200 kV.

$A\beta 42$ Neurotoxicity Rescue. $A\beta 42$ Preparation. $A\beta 42$ (purchased from Keck lab) treated with HFIP (hexafluoroisopropanol, Sigma 105228) followed by air-dry with speed Vac and storage at –20 °C. Dissolved HFIP treated $A\beta 42$ with 10% of 20 mM of NaOH in phosphate buffered saline (PBS) and determined $A\beta 42$ concentration by measuring the absorbance at λ 214 nm.

Primary Cortical Neuron Preparation. Removed fetuses from pregnant C57BL/6 pregnant mouse at gestation (14 d) and isolated primary cortical neurons. Place 150 000 neuronal cells to each well in a 48-well plate (pretreated with Poly-D-Lysine) in grow media of Neurobasal media supplement with B27 supplement, Gentamycin, and glutamax (all from Life Technologies) and incubated the cells at 37 °C in the chamber (5% CO_2) for 6 d.

Assay. Primary cortical neurons were treated with A β 42 10 μ M (final concentration) and test compounds at 10, 5, 2.5, and 1.25 μ M (final concentration) in growth media of Neurobasal media supplement with B27 AO supplement. The cells treated with A β 42 were taken as positive control, the cells treated with DMSO were taken as negative control, and the cells treated with compounds only were taken as negative control. Cells were incubated at 37 °C in 5% CO₂ chamber for 4 d. Cell viability was determined using cell counting kit (CCK-8) assay after 4 d of treatment. The data were normalized and calculated as a percentage of untreated control values. Each treatment group was done in triplicate.

■ ASSOCIATED CONTENT

■ Supporting Information

Structures, energies and Cartesian coordinates for all computed compounds. This material is available free of charge via the Internet at <http://pubs.acs.org>. CCDC deposition number 1012641.

■ AUTHOR INFORMATION

Corresponding Authors

*Fax: +61393476750. Phone: +61383442555. E-mail: kbarnham@unimelb.edu.au.

*Fax: +34868884148. Phone: +34868887455. E-mail: jrui@um.es.

Notes

The authors declare no competing financial interest.

■ ACKNOWLEDGMENTS

This work was financially supported by the European Union Seventh Framework Programme—Marie Curie Cofund (FP7/2007–2013) under U-IMPACT Grant No. 267143 and the Spanish Ministerio de Economía y Competitividad and FEDER (Project No. SAF2011-26611), the Fundación Séneca-CARM (Project 15354/PI/10) and COST CM1105 for providing opportunities of discussion.

■ REFERENCES

- (1) Kenche, V. B.; Hung, L. W.; Perez, K.; Volitakes, I.; Ciccotosto, G.; Kwok, J.; Critch, N.; Sherratt, N.; Cortes, M.; Lal, V.; Masters, C. L.; Murakami, K.; Cappai, R.; Adlard, P. A.; Barnham, K. J. *Angew. Chem., Int. Ed.* **2013**, *52*, 3374.
- (2) Hardy, J.; Selkoe, D. J. *Science* **2002**, *297*, 353.
- (3) Nguyen, M.; Robert, A.; Sournia-Saquet, A.; Vendier, L.; Meunier, B. *Chem.—Eur. J.* **2014**, *20*, 6771.
- (4) Biran, Y.; Masters, C. L.; Barnham, K. J.; Bush, A. I.; Adlard, P. A. *J. Cell. Mol. Med.* **2009**, *13*, 61.
- (5) Valensin, D.; Gabbianib, C.; Messori, L. *Coord. Chem. Rev.* **2012**, *256*, 2357.
- (6) Hureau, C.; Faller, P. *Dalton Trans.* **2014**, *43*, 4233.
- (7) Barnham, K. J.; Kenche, V. B.; Ciccotosto, G. D.; Smith, D. P.; Tew, D. J.; Liu, X.; Perez, K.; Cranston, G. A.; Johanssen, T. J.; Volitakis, I.; Bush, A. I.; Masters, C. L.; White, A. R.; Smith, J. P.; Cherny, R. A.; Cappai, R. *Proc. Natl. Acad. Sci. U.S.A.* **2008**, *105*, 6813.
- (8) Rodríguez-Rodríguez, C.; Telpoukhovskaia, M.; Orvig, C. *Coord. Chem. Rev.* **2012**, *256*, 2308.
- (9) Rodríguez-Rodríguez, C.; Sánchez de Groot, N.; Rimola, A.; Alvarez-Larena, A.; Lloveras, V.; Vidal-Gancedo, J.; Ventura, S.; Vendrell, J.; Sodupe, M.; González-Duarte, P. *J. Am. Chem. Soc.* **2009**, *131*, 1436.
- (10) Choi, J. S.; Braymer, J. J.; Nanga, R. P.; Ramamoorthy, A.; Lim, M. H. *Proc. Natl. Acad. Sci. U. S. A.* **2010**, *107*, 21990.
- (11) Sharma, A. K.; Pavlova, S. T.; Kim, J.; Finkelstein, D.; Hawco, N. J.; Rath, N. P.; Kim, J.; Mirica, L. M. *J. Am. Chem. Soc.* **2012**, *134*, 6625.
- (12) Kenche, V. B.; Barnham, K. J. *Br. J. Pharmacol.* **2011**, *163*, 211.

(13) He, L.; Wang, X.; Zhao, C.; Wang, H.; Du, W. *Metallomics* **2013**, *5*, 1599.

(14) Collin, F.; Sasaki, I.; Eury, H.; Faller, P.; Hureau, C. *Chem. Commun.* **2013**, *49*, 2130.

(15) Yellol, G. S.; Donaire, A.; Yellol, J. G.; Vasylyeva, V.; Janiak, C.; Ruiz, J. *Chem. Commun.* **2013**, *49*, 11533.

(16) Lentz, C. S.; Halls, V. S.; Hannam, J. S.; Strassel, S.; Lawrence, S. H.; Jaffe, E. K.; Famulok, M.; Hoerauf, A.; Pfarr, K. M. *J. Med. Chem.* **2014**, *57*, 2498.

(17) Schiffmann, R.; Neugebauer, A.; Klein, C. D. *J. Med. Chem.* **2006**, *49*, 511.

(18) Tsukamoto, G.; Yoshino, K.; Kohno, T.; Ohtaka, H.; Kagaya, H.; Ito, K. *J. Med. Chem.* **1980**, *23*, 734.

(19) Zimmermann, G.; Papke, B.; Ismail, S.; Vartak, N.; Chandra, A.; Hoffmann, M.; Hahn, S. A.; Triola, G.; Wittinghofer, A.; Bastiaens, P. I.; Waldmann, H. *Nature* **2013**, *497*, 638.

(20) Ong, J. X.; Yap, C. W.; Ang, W. H. *Inorg. Chem.* **2012**, *51*, 12483.

(21) Ginzinger, W.; Mühlgassner, G.; Arion, V. B.; Jakupec, M. A.; Roller, A.; Galanski, M.; Reithofer, M.; Berger, W.; Keppler, B. K. *J. Med. Chem.* **2012**, *55*, 3398.

(22) Noël, S.; Cadet, S.; Gras, E.; Hureau, C. *Chem. Soc. Rev.* **2013**, *42*, 7747.

(23) (a) Spek, A. *Acta Crystallographica Section D* **2009**, *65*, 148–155.

(b) Spek, A. L. *PLATON – A multipurpose crystallographic tool*; Utrecht University: Utrecht, The Netherlands, 2005.

(24) Janiak, C. *J. Chem. Soc., Dalton Trans.* **2000**, 3885.

(25) Yang, X. J.; Drepper, F.; Wu, B.; Sun, W. H.; Haehnel, W.; Janiak, C. *Dalton Trans.* **2005**, 256. and supplementary material therein.

(26) Price, J. H.; Williamson, A. N.; Schramm, R. F.; Wayland, B. B. *Inorg. Chem.* **1972**, *11*, 1280.